TECHNICAL MEMORANDUM

ANL-CT-80-23

SOME BASIC CONSIDERATIONS AND POSSIBLE IMPROVEMENTS ON THE SOLAR POND

by

W. T. Sha, Y. S. Cha,
K. V. Liu, and S. L. Soo

Components Technology Division

ARGONNE NATIONAL LABORATORY

June 1980

Prepared for the
U. S. DEPARTMENT OF ENERGY
Under Contract W-31-109-Eng-38

DISCLAIMER

Printed in the United States of America
Available from
National Technical Information Service
U. S. Department of Commerce
5285 Port Royal Road
Springfield, VA 22161

NTIS price codes
Printed copy: A04
Microfiche copy: A01

Dr. 2222

TECHNICAL MEMORANDUM

ANL-CT-80-23
Solar Thermal—
Total Energy Systems
(UC-62a)

Master

ARGONNE NATIONAL LABORATORY
9700 South Cass Avenue
Argonne, Illinois 60439

SOME BASIC CONSIDERATIONS AND POSSIBLE IMPROVEMENTS ON THE SOLAR POND

by

W. T. Sha, Y. S. Cha, K. V. Liu, and S. L. Soo*

Prepared by

Components Technology Division

June 1980

*Consultant, University of Illinois

THIS PAGE

WAS INTENTIONALLY

LEFT BLANK

TABLE OF CONTENTS

LIST OF FIGURES

ABSTRACT

Experimental results were compared to theoretical stability criteria of a salt gradient solar pond. Cellular motion in the non-convective layer is expected. Innovative concepts on friction stabilization using stabilizing barriers and longitudinal stratification to improve pond heat extraction efficiency are presented.

I. INTRODUCTION

The feasibility of solar ponds has been amply demonstrated by various field units (Weinberger 1964, Nielsen 1976, 1978, 1979; Nielsen and Rabl 1978; Dickinson, Clark and Iantuono, 1976), and an experimental and analytical study of Zangrando (1979). A number of theoretical analyses have been reported on the stability of the double diffusive or nonconvective layer of the pond (Veronis, 1968; Baines and Gill, 1969; Turner, 1968; Nield, 1967; to name a few). However, very little efforts toward correlation of experimental results and theoretical analysis have been made. The work of Zangrando is the first of its kind.

II. STABILITY CRITERIA

The above cited theoretical analysis and ours (Lin, Sha and Soo 1979) for both 2- and 3-dimensional stability gave: (case F* = 0 in Appendix A)

$$R_a = \frac{Pr + k}{Pr + 1} R_c + (1 + k)\left(1 + \frac{k}{Pr}\right)\frac{27\pi^4}{4} \qquad (2.1)$$

where R_a and R_c are the thermal and salinity Rayleigh numbers, respectively

$$R_a = g\alpha_T \Delta T d^3/\kappa_T \nu \qquad (2.2)$$

$$R_c = g\alpha_c \Delta C d^3/\kappa_T \nu \qquad (2.3)$$

Pr is the Prandtl number (ν/k_T), $k = \kappa_c/\kappa_T$, κ_c, κ_T are the salinity and thermal diffusivities, respectively, g is the gravitational acceleration, ν is the kinematic viscosity, d is the depth of the layer, α_T is the coefficient of thermal expansion, α_c is that for solutal expansion, $\Delta C = C_{bottom} - C_{top}$ for concentration C, and $\Delta T = T_{bottom} - T_{top}$ for temperature. Equation (2.1) applies to positive values of R_a and R_c and for free boundaries. This relation is shown in Fig. 1 by a solid line.

Figure 1 also includes the theoretical results of Elder (1969) as marked. His results were expressed in R_a vs. $\gamma = R_c/R_a$ and he identified overstable ranges for cases with or without boundaries and convective overturning. His results can be considered the first one suggesting introducing walls to improve stability. His results are in general agreement with Veronis

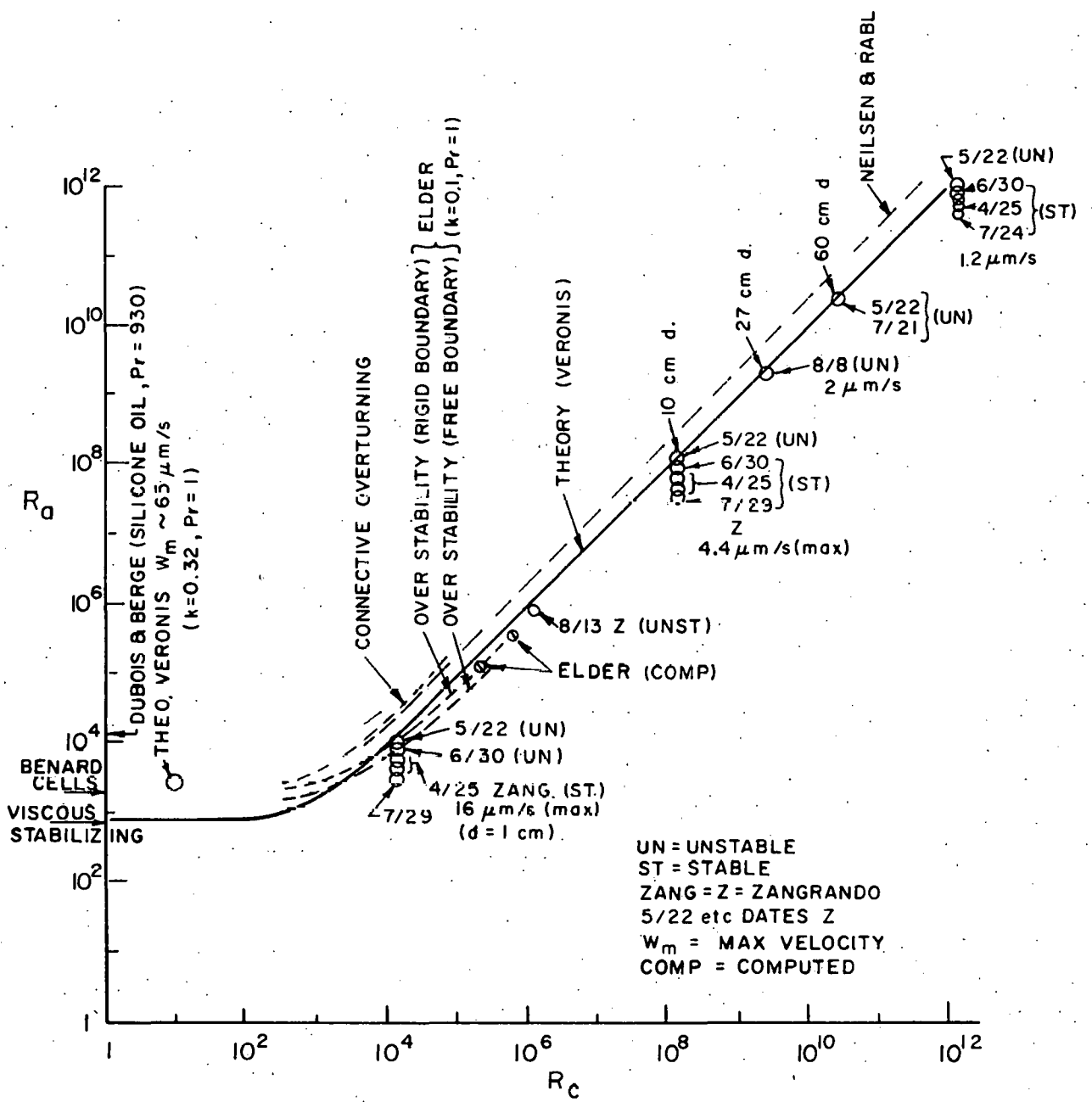

Fig. 1. Comparison of Various Theoretical and Experimental Results Concerning Stability of a Solar Pond (k = 0.02, Pr = 3.54)

(1968) and others in terms of Eq. (2.1). He demonstrated that, depending on length-thickness relations, the cellular structure of unstable motion tends to breakup as shown in Fig. 2. Cases of calculated results are also shown in Fig. 1, noting a maximum velocity w_m of 65 μm/s obtained by Veronis (1968) and the results of Elder (1969) for $R_a = 3 \times 10^5$ and 10^6. The dashed line showing Nielsen and Rabl's (1976) criterion for shrinking convection layer which has been converted to the form:

$$R_a < \frac{Pr + k}{Pr + 1} k^{1/3} R_c - 10^3 \qquad (2.4)$$

is also included in Fig. 1. Its significance is unclear when comparison is made to the experimental data.

Other theoretical limits shown are the Benard cells at $R_c = 0$ with $R_a = 1708$ (Dubois and Berge, 1978). Viscous stabilizing at $R_a = 657.5$ is also indicated.

III. COMPARISON WITH EXPERIMENTAL DATA

Detailed measurements in solar ponds are few. Zangrando's (1979) measurements and computations constitute the only source of detailed data at this time. Stability conditions were observed from measurements of temperature and salinity distributions over the depth and computations of velocities from the measured temperatures and concentrations. Figure 1 shows Zangrando's results in terms of stability ("ST" for stable nonconvective layer and "UN" for unstable layer) on various dates. We note that the range between stable and unstable operations are rather close and in general, a stable layer calls for a lower R_a than R_c. Conversion from Zangrando's data in Appendix B include: $k_1 = PrR_a/(Pr + k)(1 + k)$; $k_2 = PrR_c/(Pr + 1)(1 + k)$; $w = k_T w^*/d$ (notations in Appendix A), w^* is W in Zangrando.

We note that all operating points of Zangrando's solar pond are close to the stability curve of Veronis. Instability occurs for operation near the stability curve over the whole range of $R_a = 10^4$ to $R_a = 10^{12}$ with layers of 1 cm to 100 cm thick. The maximum velocity of fluid motion ranges from 16 μm/s for d = 1 cm, to 4.4 μm/s for d = 10 cm, to 1.2 μm/s (nonconvergent result) for d = 100 cm. Comparable quantities in other studies are 65 μm/s in Veronis' (1968) computation (Pr = 1) and Dubois and Berge (1978) who gave 337 μm/s for silicone oil (Pr = 930)(d = 1 cm). It appears that velocities in

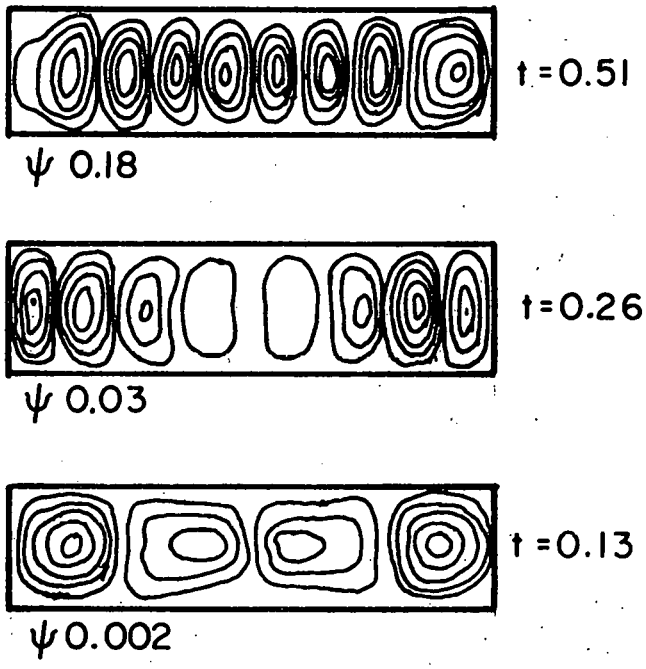

Fig. 2. Distribution of ψ as Successive Times Showing Change in Horizontal Wave - Number Associated with Delayed Instability

$$\tau = t_r \kappa_T / d^2, \quad \psi = \psi_r / \kappa_T$$

Subscript r for real quantities, ψ_r is the stream function (Elder 1969).

units of 10 μm/s is common in the motion in the nonconvective double diffusive layer. The low velocities in the case of thick layers suggest that the motion may have broken up into small cellular motions in analogy to that in turbulent shear motion as illustrated in Fig. 3 (Corrsin and Kollmann, 1977, as an analogy). Solution as in Fig. 3 is obtainable from computation of three dimensional cellular velocity field under constant gradients.

IV. POSSIBLE IMPROVEMENTS

It is seen that a conventional solar pond may undergo transition from stable to unstable condition by the perturbation of the concentration gradient whose adjustment lags behind that of temperature gradient. Even in the absence of extensive data, the agreement between experimental results and theoretical stability criterion of Veronis can be considered assuring in the preliminary sense (Fig. 1). The basic mode of circulation is not likely to be sustained in a layer 1 m deep; rather cellular motion is expected. An improvement is analyzed from consideration of the fundamental relations.

A. Stabilizing Barriers

Assuring a stable non-convective gradient layer of a solar pond is vital to its energy efficiency. Reducing the loss of salt due to mixing reduces salt replenishment cost and energy or land area for salt regeneration.

The barriers are constituted by a vertical grid-work of transparent plastic sheets open at the top and bottom as shown in Fig.4. Figure 5 shows that such a grid-work is readily formed by gluing sheets at joints and stretched by mooring cords as in Fig. 4. Figure 6 shows the barrier in place.

The top layer is open to all vertical channels. Clear water rinse (natural or artificial) can be applied as in conventional solar ponds.

The non-convective layer is now subdivided into vertical channels. Convection cells may take the form as shown in Fig. 6. In this way, large scale unrestricted convective motion is reduced by wall friction of the barriers and by reduced cell motion. The effect of motion induced by the sloping walls is isolated to only the vicinity of the wall.

Practical dimensions of the barriers will be: for a depth (d, Fig. 6) of 0.5 m, the width (w, Fig. 5) should be 5 to 10 cm. Equalizing perforations might be provided at 10 to 20 cm intervals along the sides (Fig. 4) with holes of 3 to 5 mm diameter. The characteristic dimension for the Rayleigh number will be based on the width w.

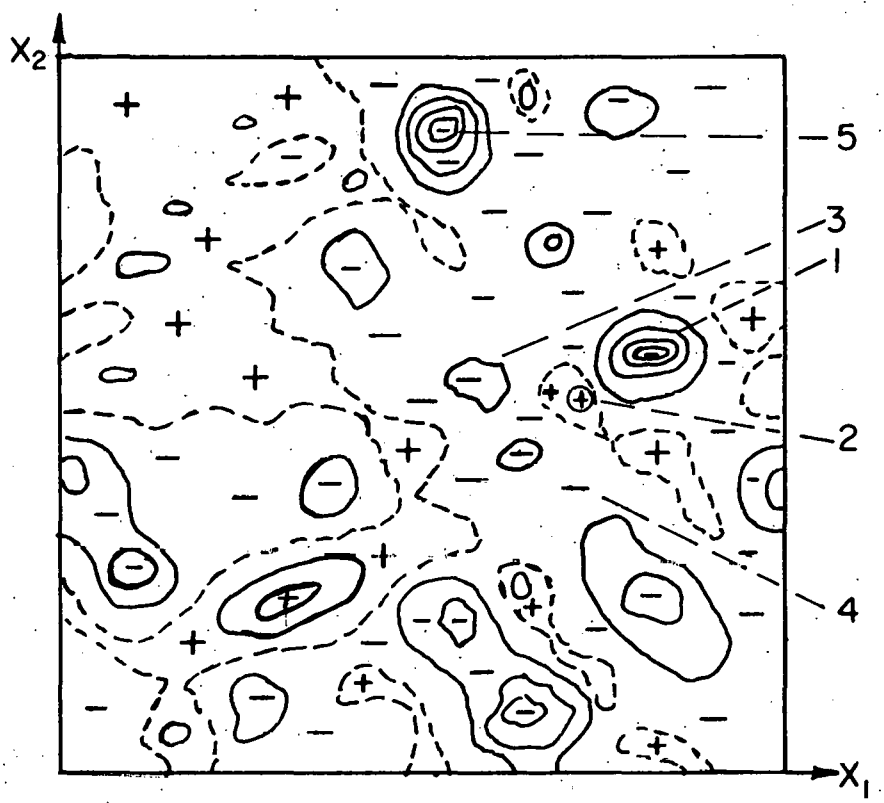

$p \frac{\partial u_i}{\partial x_1}$ IN PLANE $x_3 = 0.5$ $\frac{\partial u_1}{\partial x_1} > 0$ +

TIME $t = 0.2$

MEAN SHEAR $\frac{d\bar{U}_1}{dx_2} = 3.5$ $\frac{\partial U_1}{\partial x_1} < 0$ -

Fig. 3. Cellular Structure in Turbulent Shear Motion (Corrsin and Kollmann 1977)

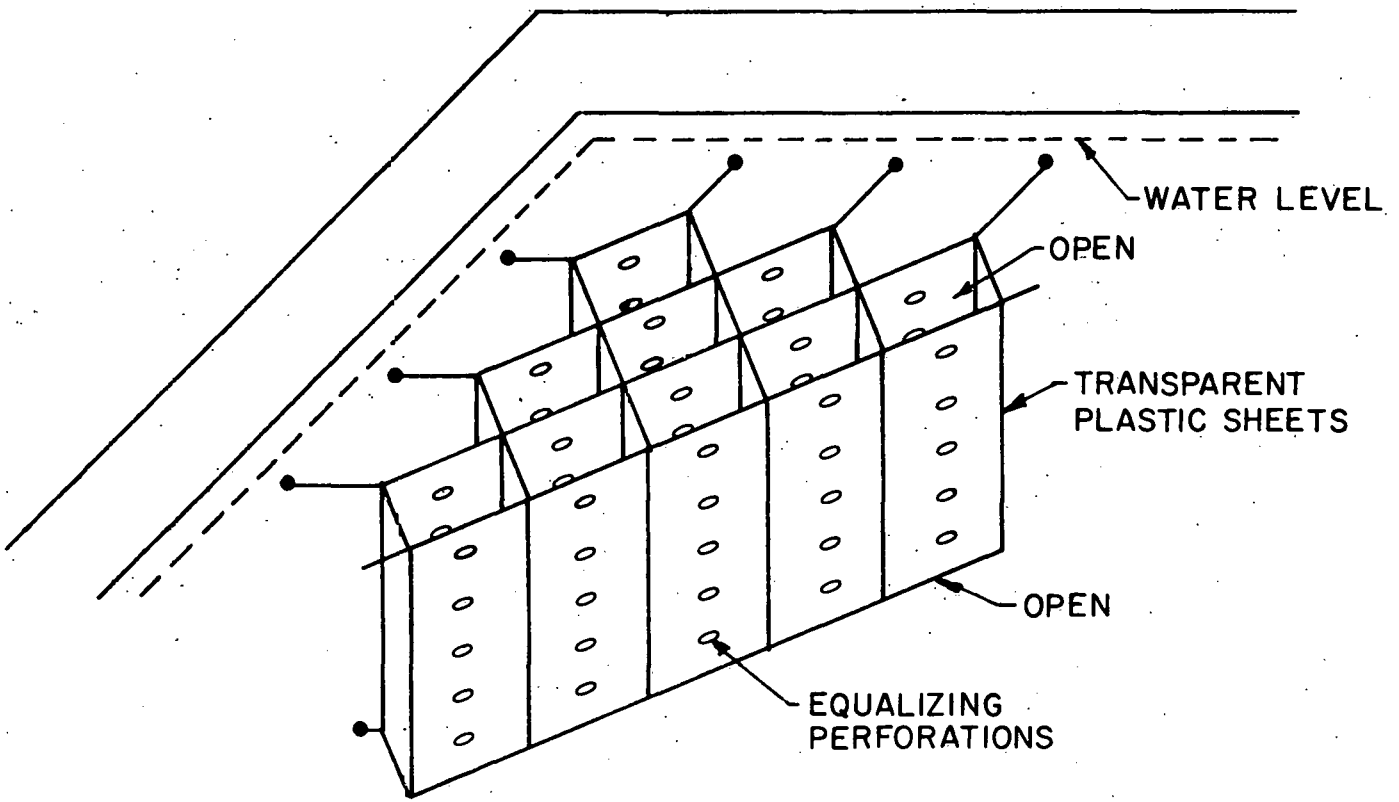

Fig. 4. Stabilizing Barrier

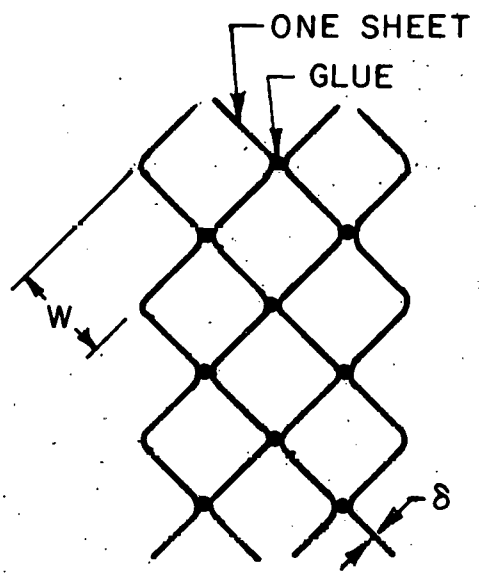

Fig. 5. Forming Elements of Barrier

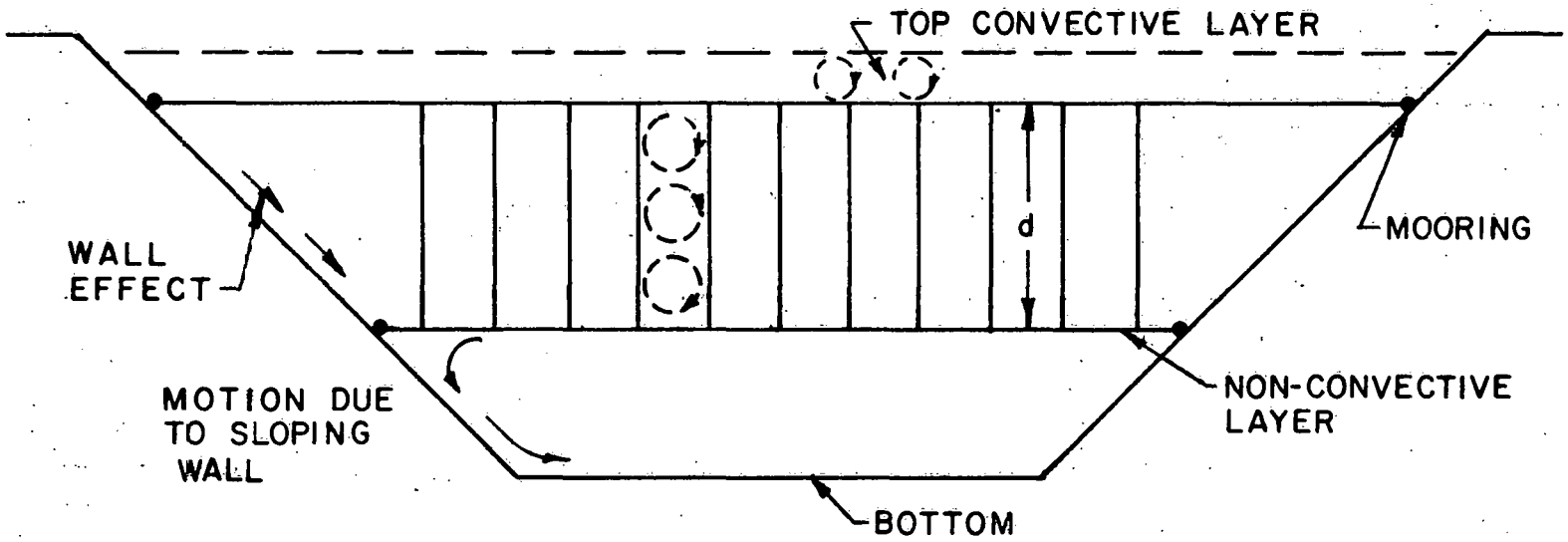

Fig. 6. Deployment of Barriers

Filling of the pond should proceed from the bottom by introducing saline water of gradually decreasing concentration.

Presence of the barriers reduces mixing by wind over the pond by dissipating the induced liquid motion and waves. Reduced effect of wind shear is seen from the experimental results of Kato and Phillips (1969) and Wyatt (1978). Increased flow resistance by the barriers reduces the effect of heavy rain and hail storms. Active top skimming and draining would be sufficient.

Heat and salt loss by convection to the top convective layer is expected to be greatly reduced (Linden and Shirtcliffe, 1978) by a significant decrease in R_a because of the presence of the barriers.

B. Friction Stabilization of Non-convective Layer

It is seen that the viscous stabilized region in the stability diagram of the non-convective layer can be extended by deliberately introducing friction elements in that layer. This can be accomplished by rods or thin sheets of plastic forming a grid-work.

To analyze the basic relations, the basic equations of Veronis (1968) were modified by introducing the friction term (Soo, 1967).

$$F^* = F\, d^2/\kappa_T \tag{4.1}$$

where F is the inverse relaxation time for momentum transfer from the wall of the friction element to the fluid; d is the depth of the nonconvective layer, and κ_T is the thermal diffusivity. Based on the analysis in Appendix A, the criteria of Veronis are modified to: $\left(b^2 = \frac{3}{2}\pi^2\right)$

$$R_a = \left(R_c/k\right) + \left(27\pi^4/4\right)\left(1 + F^* \frac{2}{3\pi^2}\right) \tag{4.2}$$

and

$$R_a = \frac{Pr + k + F^*\,(2/3\pi^2)}{Pr + 1 + F^*\,(2/3\pi^2)} R_c + (k+1)\left(1 + \frac{k}{Pr}\right)\frac{27\pi^4}{4} + F^*\left(9\pi^2/2\right)\frac{1 + \frac{1+2k}{Pr} + \frac{k+1}{Pr} F^*\left(2/3\pi^2\right)}{1 + Pr + F^*\left(2/3\pi^2\right)} \tag{4.3}$$

which reduces to the results of Veronis (1965) for $F^* = 0$.

When plotted in the same R_a vs. R_c diagram, Eq. (4.3) gives the relation in Fig. 7. We noted that even at $R_c = 0$, stable non-convective layer is maintained for R_a below the following values:

$F^*(2/3\pi^2)$	R_a
100	1.96×10^4
10	2.56×10^3
1	1.12×10^3
0.1	693.2
0	657.5

To achieve these values of F^*, we note that from Appendix A:

$$F^* = 8\ (d^2/w^2)(\nu/\kappa_T) \qquad (4.4)$$

which for transparent plastic sheets of $\delta \sim 100$ μm, w = 10 cm, d = 0.5 m, $F^* \sim 600$ or $F^*(2/3\pi^2) \sim 40$. That is, a stable non-convective layer may conceivably be maintained even when salt is absent. This is seen to be a way toward an even more economical solar pond system by eliminating the need for the salt and the liner. The use of membranes was also suggested by Hull (1980).

In practice, it is expected that some salt or other additive such as bleaching powder will be needed to prevent the growth of algae in fresh water. However, smaller concentrations of salt might be used and the environmental effects due to leakage might be lessened.

C. Utilization of Water from Bottom Convective Layer

In many cases, heat exchanger tubes are immersed in the bottom convective layer (Nielsen 1979) and another mode is to take out hot water from the bottom and return it at the top of that layer (Zangrando 1979) with the aim of mixing. It appears, however, that available energy can be increased from these modes by using a longitudinal pond (say 40 m x 100m for a one-acre pond) by taking out hot water from one end of the length of the pond and return cold water near the bottom at the other end, and to maintain a longitudinal stratification. For example (Appendix C), consider a pond with a 2 m deep bottom convection layer which stores heat from spring to summer to raise 2 million gallons of water to 88°C and to use the heat stored to dry grains over a month period from October 1 while the ambient temperature drops from 15°C to 10°C. Heat is extracted by pumping salt water at 75 gpm to heat air in a heat exchanger. A mean velocity 59 μm/s over the pond can be achieved with suitable distributors for inlet and outlet. Numerical interpretation

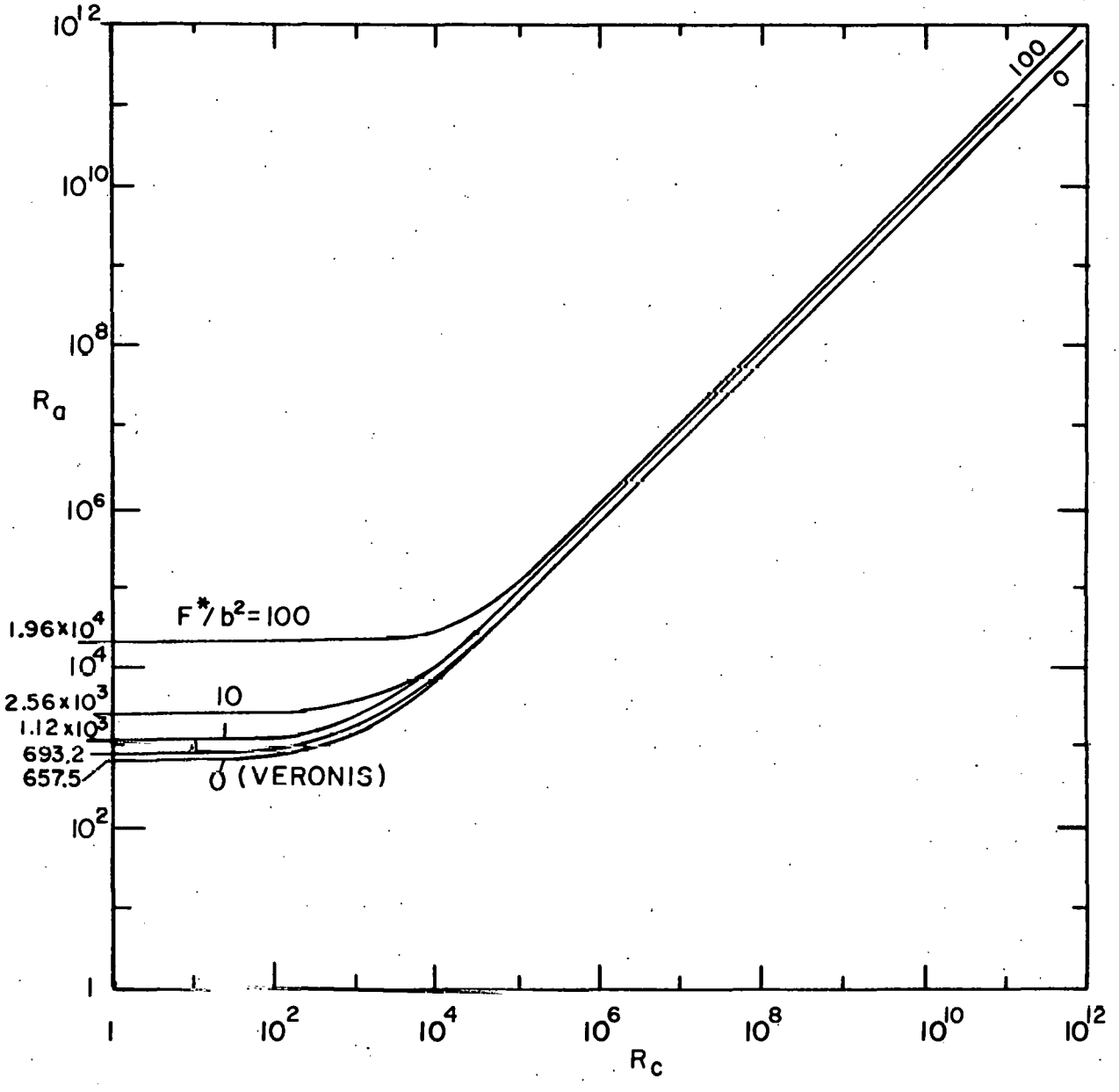

Fig. 7. Friction Stabilized Double Diffusive Layer [$b^2 = (3/2)\pi^2$]

gives the result in Fig. 8 comparing the cases of cold water returned remaining stratified and cold and hot water being mixed.

If the water remains unmixed, the original hot water would have been used up by the 19th of October with 1.82×10^9 Btu delivered for grain drying. After that date, continuing use of water at 85°F (30°C) gradually reduces to 28°C, with 0.95×10^6 Btu/hr available for heating air dropping its temperature from 12°C to 11°C; the total energy available for the last 11 days amounts to 0.26×10^9 Btu, giving a total available energy of 2.08×10^9 Btu when longitudinal stratification is maintained, vs. 1.77×10^9 Btu when the pond is completely mixed. The actual operating curve for the stratified case is seen to follow the dotted line due to diffusion of heat even when mixing is minimized.

Even in the stratified mode of operation, the mixing layer thickness is expected to grow to 1.7 m over this one month period. If the extraction is spread over a year, this mixing layer will grow to 5.5 m. Further details and stability will be treated in the next section. It suffices to point out here that the mean velocity due to extraction of hot water from the bottom convection layer will be similar in magnitude to that of the thermal haline induced motion. This further confirms the desirability of the barriers in Sec. IV.A.

V. STABILITY OF EXTRACTION

The greatest amount of available energy from a solar pond is seen to be attained by longitudinal extraction. This is accomplished by taking hot water from one end of a long storage pond (Fig. 9) (say 100m x 40m) via a distributor and return the cold water after use to the other end, again via a distributor to insure low velocity and to avoid mixing. For a pond of 2m convective layer depth of the above width of 100m, at an extraction rate of 75 gpm, say, the mean flow velocity will be 23.7 μm/s, or 2.05 mm/day. Note that such a velocity is lower than and is of the same order as that due to convection in the gradient layer, and therefore, will not disturb the gradient layer. Our concern is, however, in the stability of the hot water-cold water boundary and whether significant mixing besides natural diffusion would take place. Instability may occur due to disturbances because of inertial force produced by different densities of fluids.

For the system in Fig. 9, whose actual length (L) to thickness (h) ratio may range from 50 to 100, returned cold water will not simply slide under the

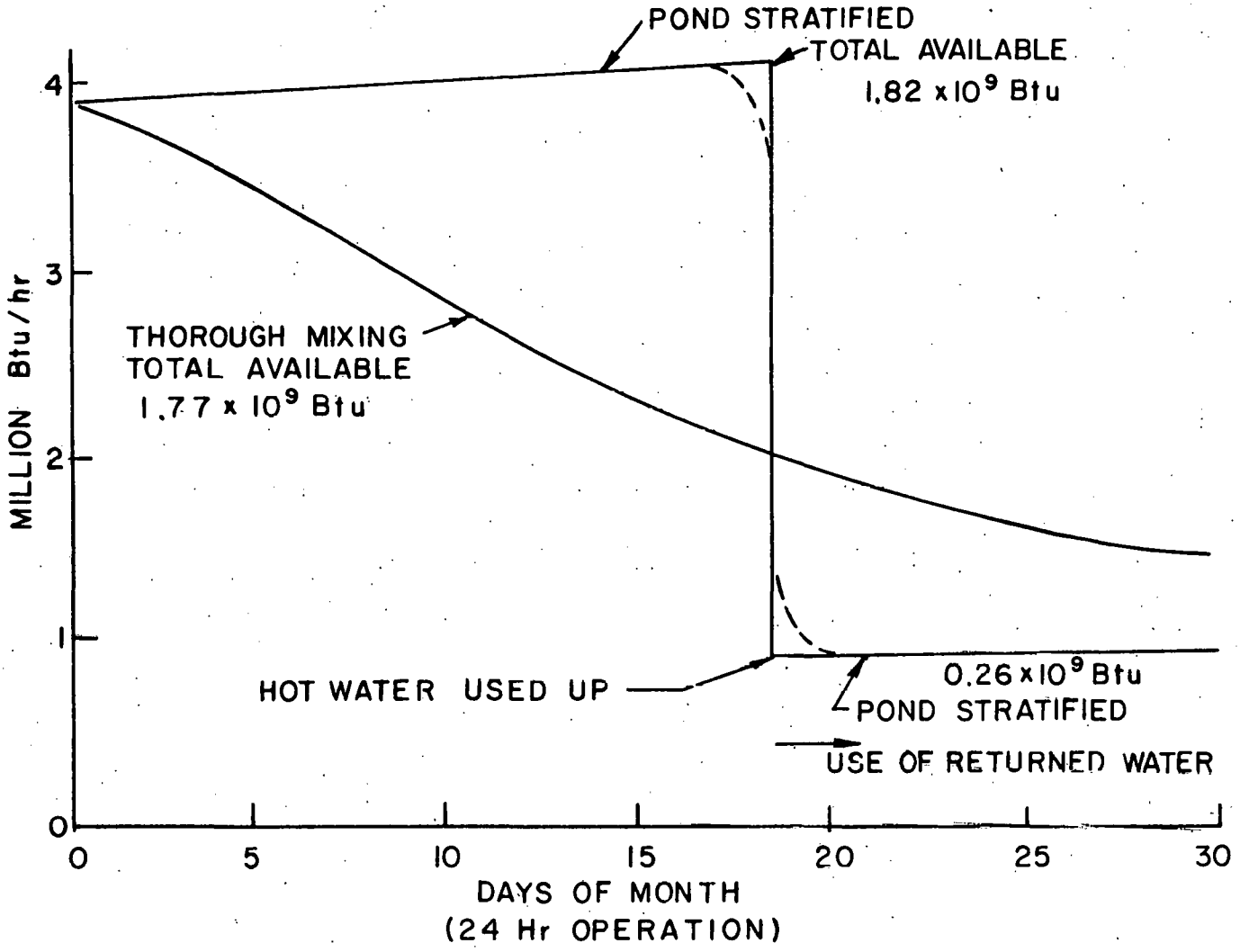

Fig. 8. Advantage of Longitudinal Stratification in a Pond
Total Available for Stratified Pond 2.08 x 10^9 Btu

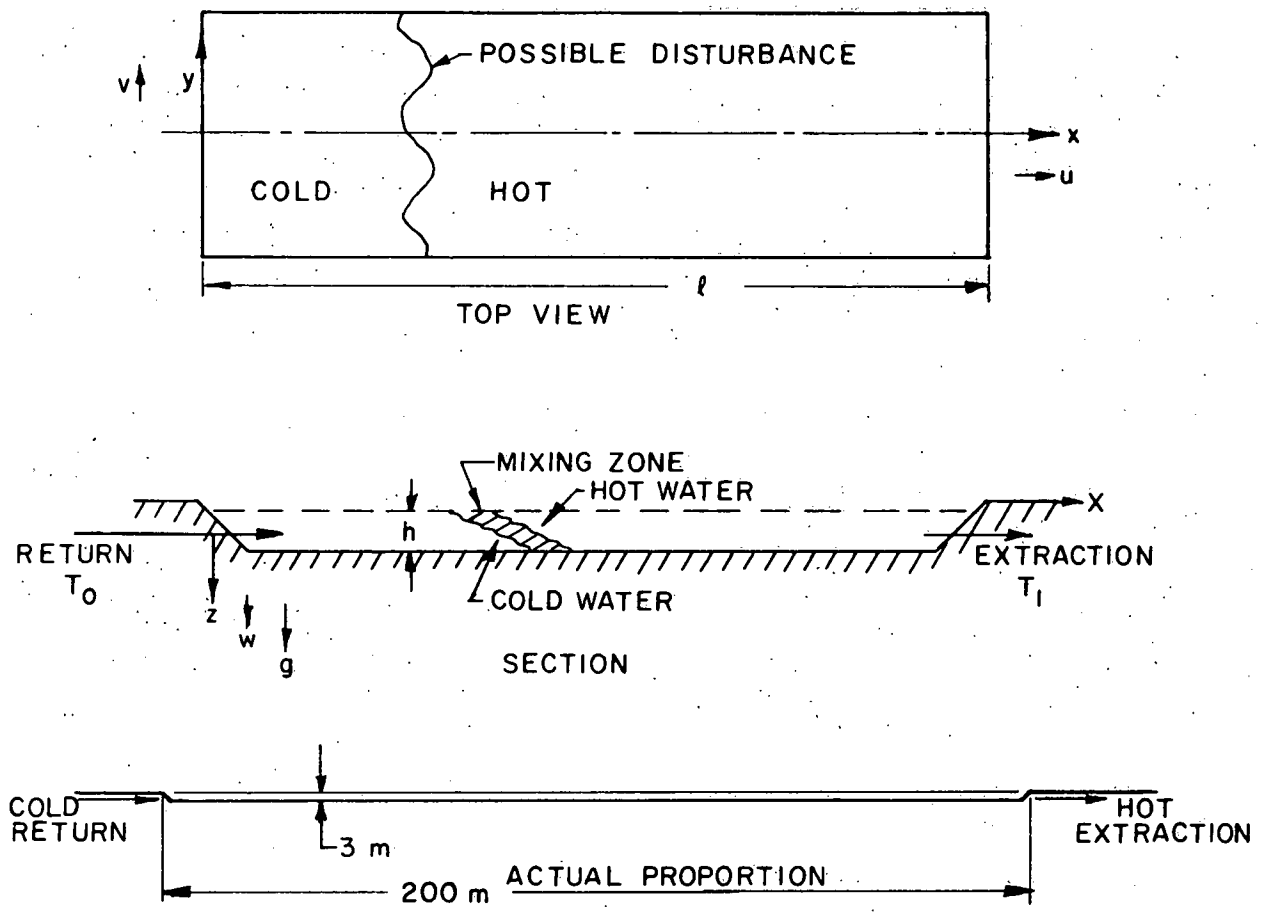

Fig. 9. Coordinates for Analyzing Stability of Extraction (Top Figures in Exaggerated Scale, Actual $L/h \sim 50$ to 100)

hot water because of viscous resistance to flow of a thin cold layer under the hot fluid (see, e. g. Yih 1965 for fundamentals of stratified flow), with mixing by diffusion. The trend will actually be represented as in Fig. 9, for the distribution of hot and cold water at a finite extraction rate. The system can therefore be represented by a two-dimensional model in a preliminary study.

To explore the stability of extraction in terms of transverse disturbance, we take the system as shown in Fig. 9. The cold fluid returns at temperature T_o at a mean flow velocity u_o, displacing hot water at T_1. Possible disturbance arises from perturbation by the inertia forces. The density varies according to

$$\rho = \rho_o[1 - \alpha(T - T_o)] \qquad (5.1)$$

where ρ is the density, ρ_o is that at temperature T_o, α is the coefficient of thermal expansion, and T is the temperature of the fluid.

A. Temperature Distribution in Longitudinal Stratification

First we treat the stable longitudinal temperature distribution in a solar pond produced by diffusion at the interface of cold (at temperature T_o) and hot water (at temperature T_1). We treat this sheet of liquid of 2m (depth = h) x 20m (wide, y-direction) x 200m (long, x-direction) as a one-dimensional problem. In terms of dimensionless quantities:

$$x^+ = x/h, \qquad t^+ = t\,\kappa_T/h^2$$

$$u^+ = uh/\kappa_T, \qquad T^+ = (T_\ell - T_o)/(T_1 - T_o)$$

where T is the time, κ_T is the thermal diffusivity, u is the velocity in the x-direction, and T_ℓ is the water temperature at x. The boundary conditions are:

$$t^+ = 0, \qquad x^+ = 0, \qquad T^+ = 1$$

$$t^+ > 0, \qquad X^+ = 0, \qquad T^+ = 0$$

$$x^+ = \infty, \qquad T^+ = 1$$

for the energy equation:

$$\frac{\partial T^+}{\partial t^+} + u^+ \frac{\partial T^+}{\partial x^+} = \frac{\partial^2 T^+}{\partial x^{+2}} \qquad (5.2)$$

For constant u^+, Eq. (5.2) has the solution:

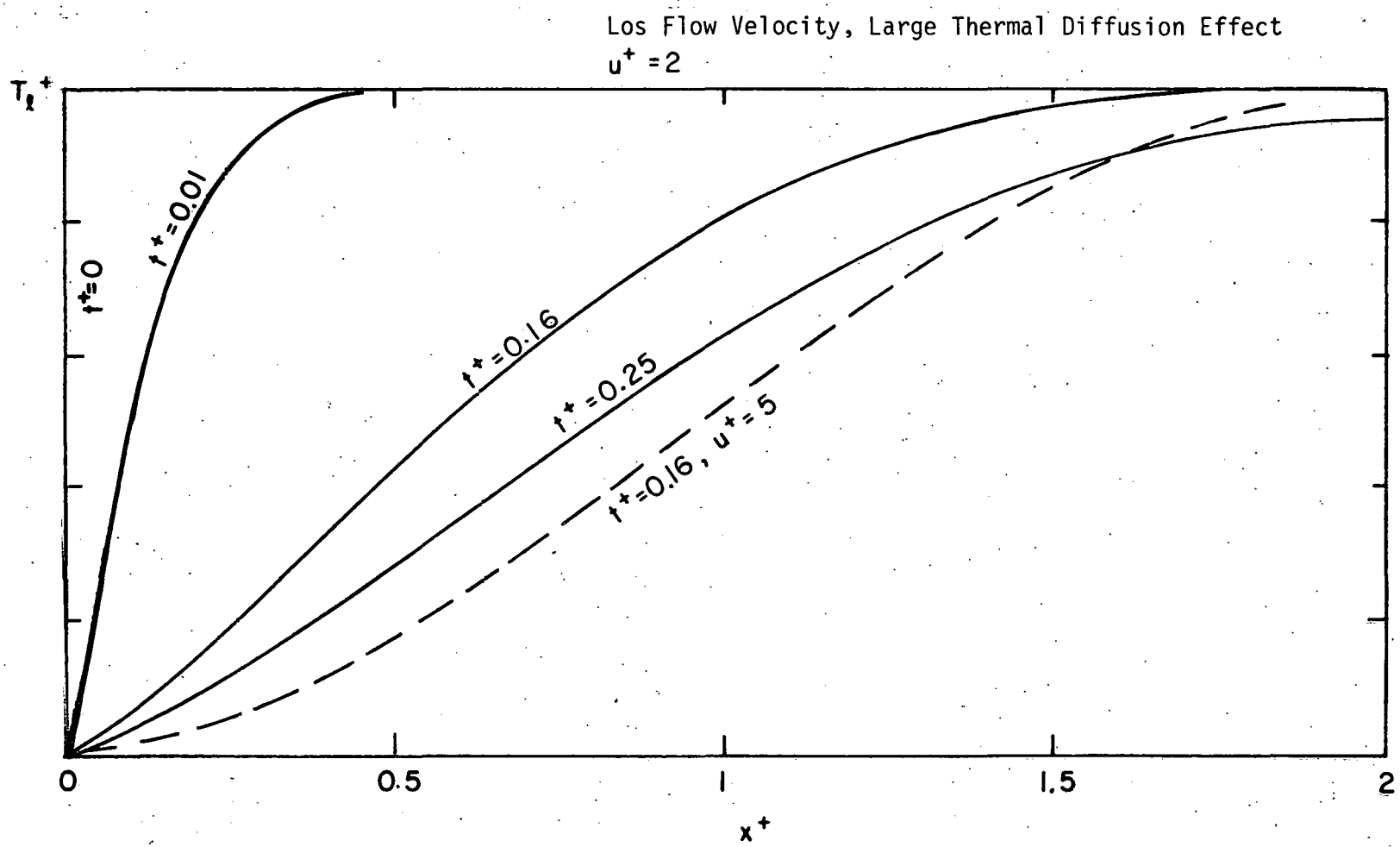

Fig. 10. Diffusion Controlled Range of Cold Water - Hot Water Interface

$$T^+ = 1 - \frac{1}{2}\left[\text{erfc}\left(\frac{x^+}{2\sqrt{t^+}} - \frac{u^+\sqrt{t^+}}{2}\right) + e^{u^+x^+}\ \text{erfc}\left(\frac{x}{2\sqrt{t^+}} + \frac{u^+\sqrt{t^+}}{2}\right)\right] \quad (5.3)$$

Equation (5.3) is plotted as shown in Fig. 10 for $u^+ = 2$ and $u^+ = 5$ at various times t^+. We note that these cases show significant effects of diffusion at low velocities. For the numerical values as cited above $u^+ = 24(\mu m/s) \times 2(m)/1.6 \times 10^{-7}\ (m^2/s) = 300$. We note that for large u^+

$$e^{u^+x^+}\ \text{erfc}\left(\frac{x^+}{2\sqrt{t^+}} + \frac{u^+\sqrt{t^+}}{2}\right) \sim \text{erfc}\left(\frac{x^+}{2\sqrt{t^+}} - \frac{u^+\sqrt{t^+}}{2}\right) \quad (5.4)$$

and the temperature distribution is approximated by, with the first boundary condition replaced by $x^+ \to -\infty$, $T^+ \to 0$,

$$T_\ell^+ = 1 - \frac{1}{2}\,\text{erfc}\left(\frac{x^+ - u^+\sqrt{t^+}}{2\sqrt{t^+}}\right) \quad (5.5)$$

which represents a diffusing interface moving at a velocity u^+t^+ and at

$$x^+ - u^+t^+ > 0 \qquad T^+ \to 1$$

$$x^+ - u^+t^+ < 0 \qquad T^+ \to 0$$

This is equivalent to a moving frame of reference at velocity u^+t^+ with the thickness of the mixing zone given by $\Delta x^+/\sqrt{t^+} = 2.74$ whence 95% of the temperature change occurs, or $\Delta x = 2.74\sqrt{t\,\kappa_T}$, Δx increases to 1.76m in a month and to 6.11m in a year. Figure 11 shows the temperature distributions at various t^+.

For later derivations, we note that

$$\partial^2 T_\ell^+/\partial x^{+2} = 0 \quad (5.6)$$

at $x^+ = u^+t^+$.

B. Basic Equations

For the present two-dimensional problem, the continuity, momentum, and energy equations take the form:

$$\frac{\partial \rho}{\partial t} + \frac{\partial \rho u}{\partial x} + \frac{\partial \rho v}{\partial y} = 0 \quad (5.7)$$

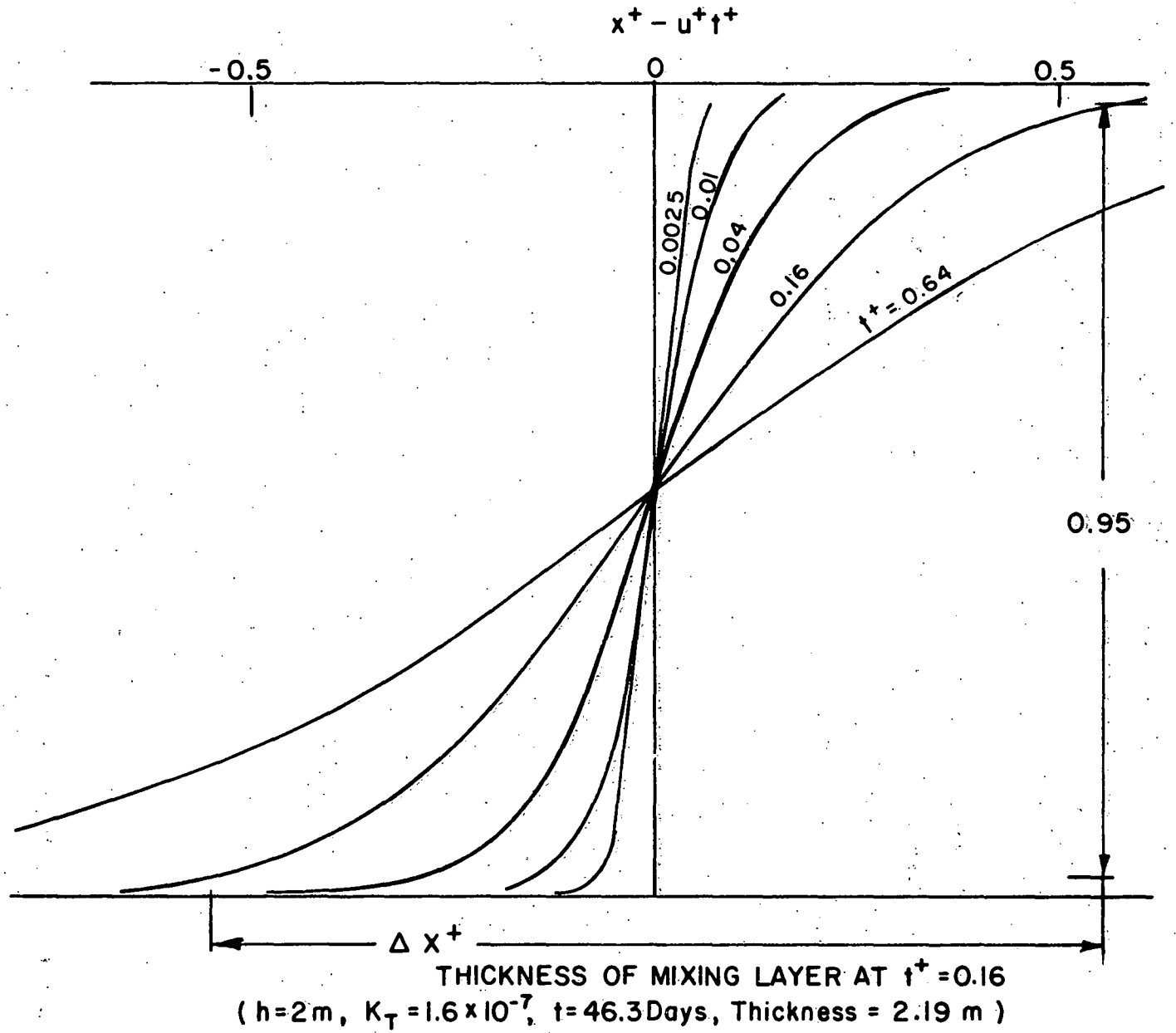

Fig. 11 Temperature Distribution in the Mixing Layer at Various Times and Positions - High Velocity, $u^+ > O[10^2]$, $t^+ > 0.0025$.

$$\rho \frac{\partial u}{\partial t} + \rho u \frac{\partial u}{\partial x} + \rho v \frac{\partial u}{\partial y} = - \frac{\partial P}{\partial x} + \mu \nabla^2 u \tag{5.8}$$

$$\frac{\partial v}{\partial t} + \rho u \frac{\partial v}{\partial x} + \rho v \frac{\partial v}{\partial y} = - \frac{\partial P}{\partial y} + \mu \nabla^2 v \tag{5.9}$$

$$\frac{\partial T}{\partial t} + u \frac{\partial T}{\partial x} + v \frac{\partial T}{\partial y} = \kappa_T \nabla^2 T \tag{5.10}$$

where t is the time, x, y are position coordinates with velocity components u, v, P is the pressure, μ is the viscosity of the fluid, and κ_T is the thermal diffusivity of the fluid.

Treating the problem as one of small disturbances, we take

$$u = u_o + u' \tag{5.11}$$

$$v = v' \tag{5.12}$$

$$P = P_o(x) + P' \tag{5.13}$$

$$\rho_o u_o = \text{constant} \tag{5.14}$$

$$T = T_\ell + T' \tag{5.15}$$

where $T_\ell(x,t)$ denotes principal longitudinal temperature distribution. With Eq. (5.1), the continuity equation yields

$$- \alpha \rho_o \frac{\partial T}{\partial t} - \alpha \rho_o u_o \frac{\partial T}{\partial x} + \rho_o \left(\frac{\partial u'}{\partial x} + \frac{\partial v'}{\partial y} \right) = 0 \tag{5.16}$$

The momentum equations become

$$\rho_o \frac{\partial u'}{\partial t} = - \frac{\partial P'}{\partial x} - \frac{\partial P_o}{\partial x} + \mu \nabla^2 u' \tag{5.17}$$

$$\rho_o \frac{\partial v'}{\partial t} = - \frac{\partial P'}{\partial y} + \mu \nabla^2 v' \tag{5.18}$$

and the energy equation is now:

$$\frac{\partial T_\ell}{\partial t} + u_o \frac{\partial T_\ell}{\partial x} = \kappa_T \frac{\partial^2 T_\ell}{\partial x^2} \tag{5.19}$$

$$\frac{\partial T'}{\partial t} + u_o \frac{\partial T'}{\partial x} + u' \frac{\partial T_\ell}{\partial x} = \kappa_T \nabla^2 T' \tag{5.20}$$

Combining Eqs. (5.17) and (5.18) gives

$$\rho_o \frac{\partial}{\partial t}\left(\frac{\partial u'}{\partial y} - \frac{\partial v'}{\partial x}\right) = \mu \nabla^2 \left(\frac{\partial u'}{\partial y} - \frac{\partial v'}{\partial x}\right) \tag{5.21}$$

This momentum equation is satisfied by velocity potential ϕ given by:

$$u' = \frac{\partial \phi}{\partial x}, \qquad v' = \frac{\partial \phi}{\partial y} \tag{5.22}$$

Eq. (5.16) becomes

$$\frac{\partial T'}{\partial t} + u_o \frac{\partial T'}{\partial x} = \frac{1}{\alpha} \nabla^2 \phi - \kappa_T \frac{\partial^2 T_\ell}{\partial x^2} \tag{5.23}$$

and Eq. (5.20) becomes

$$\frac{\partial T'}{\partial t} + u_o \frac{\partial T'}{\partial x} + \frac{\partial T_\ell}{\partial x} \frac{\partial \phi}{\partial x} = \kappa_T \nabla^2 T' \tag{5.24}$$

Equations (5.23) and (5.24) give interactions of inertia force with fluid density.

C. Stability Analysis

Equations (5.23) and (5.24) are non-dimensionalized by introducing:

$$T^+ = \frac{T' - T_p}{T_1 - T_o}, \qquad t^+ = \frac{t\kappa_T}{h^2}$$

for thickness of h (as the depth of the pond)

$$x^+ = x/h, \qquad y^+ = y/h, \qquad \phi^+ = \phi/u_o h$$

$$u^+ = \frac{u'}{u_o} = \frac{\partial \phi^+}{\partial x^+}$$

Equation (5.23) becomes

$$\frac{\partial T^+}{\partial t^+} + \frac{u_o h}{\kappa_T} \frac{\partial T^+}{\partial x^+} = \frac{u_o h}{\alpha \kappa_T (T_1 - T_\ell)} \nabla^{+2} \phi^2 - \frac{\partial^2 T_\ell^+}{\partial x^{+2}} \qquad (5.25)$$

and Equation (5.24) becomes

$$\frac{\partial T^+}{\partial t} + \frac{u_o h}{\kappa_T} \frac{\partial T^+}{\partial x^+} = - \frac{u_o h}{\kappa_T} \frac{\partial T_\ell^+}{\partial x^+} \frac{\partial \phi^+}{\partial x^+} + \nabla^{+2} T^+ \qquad (5.26)$$

Eliminating T^+ between Eqs. (5.25) and (5.26) is accomplished by applying ∇^{+2} operator to Eq. (5.25) to give

$$\left(\frac{\partial}{\partial t^+} + u_o^+ \frac{\partial}{\partial x^+} \right) \nabla^{+2} T^+ = \alpha^+ \nabla^{+4} \phi^+ - \nabla^{+2} \frac{\partial^2 T_\ell^+}{\partial x^{+2}} \qquad (5.27)$$

Substitution of Eqs. (5.25) into (5.26) for $\nabla^{+2} T^+$ and into Eq. (5.27) gives:

$$\left(\frac{\partial}{\partial t^+} + u_o^+ \frac{\partial}{\partial x^+} \right) \left(\alpha^+ \nabla^{+2} \phi^+ + u_o^+ \frac{\partial T_\ell^+}{\partial x^+} \frac{\partial \phi^+}{\partial x^+} \right)$$

$$= \alpha^+ \nabla^{+4} \phi^+ - \nabla^{+2} \frac{\partial^2 T_\ell^+}{\partial x^{+2}} \qquad (5.28)$$

where

$$u_o^+ = \frac{u_o h}{\kappa_T} , \qquad \alpha^+ = \frac{u_o h}{\alpha \kappa_T (T_1 - T_o)}$$

The last term of Eq. (5.28) is zero following Eq. (5.6).

To analyze Eq. (5.28) for stability in response to a small perturbation, we drop (+)'s for simplicity and postulate

$$\phi = \ell^{ik_x x} f(y) e^{p\tau}$$

$$\frac{\partial \phi}{\partial x} = i k_x e^{ik_x x} f(y) e^{p\tau}$$

$$\frac{\partial^2 \phi}{\partial x^2} = - k_x^2 e^{ik_x x} f(y) e^{p\tau}$$

$$\frac{\partial^2\phi}{\partial y^2} = e^{ik_x x}\frac{d^2 f}{dy^2}e^{p\tau} \equiv e^{ik_x x}\, e^{p\tau}\, D^2 f$$

$$\frac{\partial\phi}{\partial t} = e^{ik_x x}\, f(y)\, p\, e^{p\tau}$$

Equation (5.28) becomes

$$\left(p + u_o ik_x\right)\ \alpha\left(D^2 - k_x^2\right) + u_o ik_x \frac{\partial T_\ell}{\partial x}\ f = \alpha\left(D^2 - k_x^2\right)^2 f \quad (5.29)$$

Let $f = e^{ik_y y}$,

$D^2 = -k_y{}^2$,

$$D^2 - k_x{}^2 = -\left(k_x{}^2 + k_y{}^2\right) = -\,m^2$$

Equation (5.29) becomes

$$p\left[\alpha\left(-m^2\right) + u_o \frac{\partial T_\ell}{\partial x} ik_x\right] + u_o ik_x\left[\alpha(-m^2) + u_o \frac{\partial T_\ell}{\partial x} ik_x\right] = \alpha\, m^4 \quad (5.30)$$

let $p = p_r + ip_i$, the real part of Eq. (5.30) gives

$$p_r(-m^2\alpha) - p_i k_x u_o \frac{\partial T_\ell}{\partial x} - u_o^2 \frac{\partial T_\ell}{\partial x} k_x^2 = \alpha^2 m^4 \quad (5.31)$$

and the imaginary part gives

$$p_r u_o \frac{\partial T_\ell}{\partial x} k_x - p_i \alpha m^2 - u_o k_x \alpha m^2 = 0 \quad (5.32)$$

Solving for p_r from Eqs. (5.31) and (5.32) gives

$$p_r\left[m^4\alpha^2 + \left(u_o \frac{\partial T_\ell}{\partial x} k_x\right)^2\right] = -\,u_o^2 \frac{\partial T_\ell}{\partial x} k_x^2 m^2 \alpha$$

$$- \alpha^3 m^6 + u_o^2 k_x^2 \alpha m^2 \frac{\partial T_\ell}{\partial x} \quad (5.33)$$

since the [ ] term in Eq. (5.33) is always greater than zero, stable motion of the mixing front calls for the R.H.S. to be less than zero or

$$\alpha m^2 > 0$$

or, reverting to the original system of notation

$$\alpha^+ = \frac{u_o h}{\kappa_T\, \alpha\left(T_1 - T_o\right)} > 0 \quad (5.34)$$

which means that the motion is stable when the cold fluid is behind the hot fluid. Note that this checks with the Rayleigh-Taylor criterion (see Plesset, 1974).

The above is a two-dimensional analysis. If the height of the convective layer is taken into account, we expect that the stability is enhanced when the cold fluid is returned near the bottom while the hot fluid is extracted near the top of the layer.

VI. DISCUSSION

It is seen that the results of Zangrando (1979) substantiates the validity of the stability criterion of Veronis (1968) even at large Rayleigh numbers. However, all stable operations appeared to be rather close to the unstable ranges. We note that the motion due to double diffusivity has magnitudes of velocity around 50 μm/s. Withdrawal of hot water in the bottom convective layer and wind-generated motion at the surface of the pond at velocities significantly above this magnitude may lead to instability in the non-convective layer.

One possible remedy appears to be the use of a relatively large (10 cm) grid for the stabilizing barrier (Section IV.A) to isolate the nonconvective layer from disturbances in the top and bottom convective layer, the pond walls, and the withdrawal of water from the bottom layer.

Section IV.B points to the possibility of a "saltless" solar pond by using a fine transparent grid (1 cm) for the stabilizing barrier to maintain the nonconvective layer by friction alone. Although this lends hope of using any pond as a solar pond, some protection against algae growth has to be provided. In any case, this option may substantially reduce the amount of salt to be invested while paying for a viable grid system for a barrier.

Interaction of turbulent motion with the nonconvective layer occurs at the interface with the top convective layer (Wyatt 1978, Kato and Phillips 1969). However the withdrawal of the heated liquid from the bottom convective layer can be carried out, with suitable distributors, within the range of laminar motion. This aspect is currently being studied. The relation of entrainment velocity and "falling" velocity of 1 mm/day in relation to withdrawal flow (Elata and Levin 1965) calls for further clarification. We note that the "falling" velocity of 1 mm/day, if taken as the limit, then the corresponding withdrawal rate for a one-acre pond will be no more than 0.7 gpm. Most applications will call for an extraction rate on the order of ten gallons per minute for a one-acre pond. Our analysis shows that longitudinal stratification can be maintained by using suitable distributors for withdrawal from the pond and return of cold salt water to the pond. Such a measure maintains a high availability of energy from the pond. The simple case of withdrawal in the absence of solar input shows that longitudinal stra-

tification is stable. Future computer study should include simultaneous solar heating and interaction with the non-convective layer. However, stability is expected to be readily maintained.

Besides planing for experiments in a full-scale solar pond, small-scale laboratory experiments are planned for the above stabilizing barrier systems, and the withdrawal procedures.

Our aim of studying various component behavior of a solar pond is toward performing computer modeling. The aim of computer modeling of solar pond performance may be outlined as follows:

1. Correlation of parameters and formulation for a given solar pond can be carried out from the day of filling with successive corrections to sharpen the accuracy for prediction of performance and progress of a project for the purpose of evaluation or use in future designs.
2. For a state such as Illinois, if commmitted to supply farm energy via say, five thousand acres of solar pond (enough heat for all medium temperature energy needs of farms), prediction of their performance and yearly output is an important aspect of energy planning, especially against short falls in reference to weather predictions. Quantitatively (conservative estimates):

Total acres	5,000
Solar energy/acre	2×10^9 Btu/yr
Total energy	10^{13} Btu/yr
Equivalent oil	0.73×10^8 gal
Equivalent natural gas	10^4 million cu. ft.

Accurate prediction by computer will be an important aspect of the solar pond program (Energy Farming).

3. The computer model coupled with a few strategic measurements can be used for operation diagnostics, checking malfunctions and instituting corrective measures.

APPENDIX A

FRICTION STABILIZING OF NON-CONVECTION LAYER

Double-diffusive convection is a generic name given to any form of convection involving two components of different diffusivities. In the case of solar ponds, the two components are heat and salt, and the ratio of their diffusivities is about 100:1. Many other systems have also been studied; e.g., sugar-salt, and KCl-NaCl systems. Depending on the distribution of the two components in the fluid, the convection takes different forms as different mechanisms prevail. Convection occurs usually because one component is unstably distributed (i.e., it causes the density to increase upwards) which provides a source of energy for the motion, while the other component is stably distributed which acts to stabilize the motion. Two rather well-known mechanisms are the "finger" mechanism and the "diffusive" mechanism. If the component with smaller diffusivity is unstably distributed, the convection takes the form of tall, thin convection cells call "fingers". On the other hand, if the component with larger diffusivity is unstably distributed, the convection takes place in a manner similar to thermal convection, and it is called "diffusive". Photographs of both patterns can be found in the book by Turner (1973). Linear, two-dimensional stability analysis has been conducted on double-diffusive convection systems by Veronis (1968), and Baines and Gill (1969), among others. It seems not only can the results of these investigations provide insights to the solar pond behavior, but their methodologies can also be applied in analytical studies of the pond stability problem. These two-dimensional stability criteria can be readily extended to a three-dimensional system via a procedure suggested by Yih (1965) with minor modifications. The results for the three-dimensional system are discussed by Nield (1967) and a detailed derivation was presented previously (Lin et al., 1979).

The geometry of the system is defined as shown in Fig. A.1. The variation of density ρ with temperature and concentration is given by:

$$\rho = \rho_o[1 + \alpha_C(C - C_o) - \alpha_T(T - T_o)] \qquad (A-1)$$

where

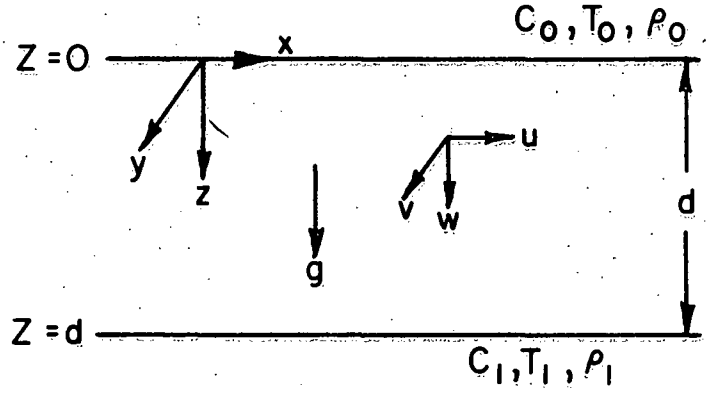

Fig. A-1. Geometry of a Double-Diffusive Convective Layer

C - concentration T - temperature

ρ - density

for which it was inferred that diffusion of solvent is negligible in a dilute solution.

The momentum equations are now modified with the above friction term:

$$\rho \frac{du}{dt} = - \frac{\partial P}{\partial x} + \mu^* \frac{\partial}{\partial x} \left(\frac{\partial u}{\partial x} + \frac{\partial v}{\partial y} + \frac{\partial w}{\partial z}\right) + \mu \nabla^2 u - \rho F u \qquad \text{(A-5)}$$

$$\rho \frac{dv}{dt} = - \frac{\partial P}{\partial y} + \mu^* \frac{\partial}{\partial y} \left(\frac{\partial u}{\partial x} + \frac{\partial v}{\partial y} + \frac{\partial w}{\partial z}\right) + \mu \nabla^2 v - \rho F v \qquad \text{(A-6)}$$

$$\rho \frac{dw}{dt} = - \frac{\partial P}{\partial z} + \rho g + \mu^* \frac{\partial}{\partial z} \left(\frac{\partial u}{\partial x} + \frac{\partial v}{\partial y} + \frac{\partial w}{\partial z}\right) + \mu \nabla^2 w - \rho F w \qquad \text{(A-7)}$$

where P is the static pressure, g is the gravitational acceleration, μ is the viscosity, and μ^* is given by $\mu^* = \zeta + (2/3)\mu$, where ζ is the bulk viscosity.

The energy equation is given by:

$$\frac{\partial T}{\partial t} + \frac{\partial}{\partial x} (uT) + \frac{\partial}{\partial y} (vT) + \frac{\partial}{\partial z} (wT) = \kappa_T \nabla^2 T \qquad \text{(A-8)}$$

where T is the temperature, and κ_T is the thermal diffusivity of the fluid.

The approximation of Linear Gradients is made as follows:

$$G_T = \frac{\partial T}{\partial z} = \frac{T_i - T_o}{d}, \quad G_C = \frac{\partial C}{\partial z} = \frac{C_i - C_o}{d} \qquad \text{(A-9)}$$

The mean temperature and mean concentration are now:

$$T_m = T_o + G_T z, \quad C_m = C_o + G_C z \qquad \text{(A-10)}$$

and the mean density is now

$$\rho_m = \rho_o \left[(1 - \alpha_T G_T z + \alpha_C G_C z)\right] \qquad \text{(A-11)}$$

which gives

$$\frac{\partial \rho_m}{\partial z} = \rho_o \left[-\alpha_T G_T + \alpha_C G_C\right] \qquad \text{(A-12)}$$

The mean static pressure and velocity components are given by:

$$\frac{\partial P_m}{\partial z} = \rho g \qquad \text{(A-13)}$$

$$u_m,\ v_m,\ w_m = 0 \tag{A-14}$$

For small perturbations from the mean quantities,

$$T = T_m + T', \quad C = C_m + C'$$

$$P = P_m + P', \quad u = u', \ v = v', \ w = w' \tag{A-15}$$

We can now proceed with the stability analyses. Equation (A-1) gives the volume dilatation as:

$$\rho - c = (\rho_o - c) - \rho_o\alpha_T(T - T_o) + \rho_o\alpha_C(C - C_o) \tag{A-16}$$

Taking total derivative with time gives

$$\frac{d}{dt}(\rho - C) = -\frac{dC}{dt} - \rho_o\alpha_T\frac{dT}{dt} + \rho_o\alpha_C\frac{dC}{dt} \tag{A-17}$$

and substitution of Eq. (A-17) into (A-4) yields

$$-(1 - \rho_o\alpha_C)\frac{dC}{dt} - \rho_o\alpha_T\frac{dT}{dt} + (\rho - C)\left(\frac{\partial u}{\partial x} + \frac{\partial v}{\partial y} + \frac{\partial w}{\partial z}\right) = 0 \tag{A-18}$$

For the first order of perturbation, C_m, T_m are independent of t. Eq. (A-18) thus gives

$$\frac{\partial u'}{\partial x} + \frac{\partial v'}{\partial y} + \frac{\partial w'}{\partial z} = 0 \tag{A-19}$$

With the assumption that $C - C_o$ is small compared to ρ_o, Eqs. (A-5) - (A-7) then become:

$$\rho_o\frac{\partial u'}{\partial t} = -\frac{\partial P'}{\partial x} + \mu\nabla^2 u' - \rho F u' \tag{A-20}$$

$$\rho_o\frac{\partial v'}{\partial t} = -\frac{\partial P'}{\partial y} + \mu\nabla^2 v' - \rho F v' \tag{A-21}$$

$$\rho_o\frac{\partial w'}{\partial t} = -\frac{\partial P'}{\partial z} + \mu\nabla^2 w' + g\rho_o(-\alpha_T T' + \alpha_C C') - \rho F w' \tag{A-22}$$

where use has been made of Eq. (A-13). Equation (A-8) becomes after dropping

higher order terms than first in (') quantities:

$$\frac{\partial T'}{\partial t} - \kappa_T \nabla^2 T' = - w' \frac{\partial T}{\partial z} = - w' G_T \qquad \text{(A-23)}$$

Also, Eq. (A-3) becomes:

$$\frac{\partial C'}{\partial t} - \kappa_C \nabla^2 C' = - w' \frac{\partial C'}{\partial z} = - w' G_T \qquad \text{(A-24)}$$

The reduction of momentum equations follows a different route as that of Veronis (1968). When expressed in vectorial form, the momentum equations (A-20) to (A-22) are represented by:

$$\frac{\partial \underline{v}'}{\partial t} = - \frac{1}{\rho_o} \nabla P' + \nu \nabla^2 \underline{v}' - \underline{k} g \alpha_T (G_T z + T') + \underline{k} g \alpha_C (G_C z + C') - F \underline{v}'$$

Application of divergence operator to both sides gives, with Eq. (A-19):

$$\frac{\partial}{\partial t} \nabla . \underline{v}' = 0 = - \frac{1}{\rho_o} \nabla^2 P' + \nu \nabla^2 \underline{v}' - \underline{\kappa} g \alpha_T \frac{\partial T'}{\partial z} + \underline{\kappa} g \alpha_C \frac{dC'}{dz} - F \nabla \cdot \underline{v}'$$

Taking derivative $\partial/\partial z$ further gives:

$$0 = - \frac{1}{\rho_o} \frac{\partial}{\partial z} \nabla^2 p' - g \alpha_T \frac{\partial^2 T'}{\partial z^2} + g \alpha_C \frac{\partial^2 C'}{\partial z^2} \qquad \text{(A-25)}$$

The pressure terms can be eliminated by applying the Laplacian operator to Eq. (A-22), resulting in:

$$\frac{\partial}{\partial t} \nabla^2 w' = - \frac{1}{\rho_o} \frac{\partial}{\partial z} \nabla^2 P' + \nu \nabla^2 \nabla^2 w' - F \nabla^2 w' - g \alpha_T \nabla^2 T' + g \alpha_C \nabla^2 C' \qquad \text{(A-26)}$$

and by a substitution of Eq. (A-25), we get

$$\left(\frac{\partial}{\partial t} + F - \nu\nabla^2\right) \nabla^2 w' = - g\alpha_T \left(\frac{\partial^2}{\partial x^2} + \frac{\partial}{\partial y^2}\right) T' + g\alpha_C \left(\frac{\partial^2}{\partial x^2} + \frac{\partial^2}{\partial y^2}\right) C' \qquad \text{(A-27)}$$

Equations (A-23), (A-24), and (A-27) are now the equations of double-diffusive convection with internal friction. Equation (A-27) differs from Yih (1965) by the signs on the right-hand side. The boundary conditions are:

$$u', v', w' = 0 \text{ at the boundaries,}$$

$$w' = 0, \quad \partial w'/\partial z = 0 \text{ at } z = 0 \text{ and } z = d$$

because of Eq. (A-19).

Elimination of P' between Eqs. (A-20) and (A-21) gives

$$\left(\frac{\partial}{\partial t} + F - \nu\nabla^2\right)\left(\frac{\partial v'}{\partial x} - \frac{\partial u'}{\partial y}\right) = 0$$

and

$$\frac{\partial v'}{\partial x} - \frac{\partial u'}{\partial y} = 0$$

means irrotational flow in the x–y plane. For velocity potential ϕ with

$$u' = \partial\phi/\partial x, \quad v = \partial\phi/\partial y$$

and with Eq. (A-19)

$$\frac{\partial^2\phi}{\partial x^2} + \frac{\partial^2\phi}{\partial y^2} = \frac{\partial u'}{\partial x} + \frac{\partial v'}{\partial y} = - \frac{\partial w'}{\partial z} \qquad \text{(A-28)}$$

which can be solved with $\phi = 0$ at $z = 0$ and d; and u, v = 0 at the boundaries are satisfied.

The dimensionless forms of the linearized three-dimensional equations are, with $F^* = Fd^2/\kappa_T$

$$\frac{1}{Pr}\frac{\partial}{\partial \tau} + \frac{F^*}{Pr} - \nabla^2 \quad \nabla^2 w^* = - R_a \quad \frac{\partial^2}{\partial X^2} + \frac{\partial^2}{\partial Y^2} \quad T^* + R_c \quad \frac{\partial^2}{\partial X^2} + \frac{\partial^2}{\partial Y^2} \quad C^* \qquad \text{(A-29)}$$

$$\left(\frac{\partial}{\partial \tau} - \nabla^2\right) T^* = - w^* \qquad \text{(A-30)}$$

$$\left(\frac{\partial}{\partial \tau} - k\nabla^2\right) C^* = - w^* \qquad \text{(A-31)}$$

The boundary conditions at Z = 0, 1 are given by

$$w^* = 0, \quad \partial w^*/\partial Z = 0, \quad T^* = S^* = 0$$

where $k = \kappa_C/\kappa_T$, $\tau = t\,\kappa_T/d^2$ = dimensionless time

$X, Y, Z = x/d, y/d, z/d$ = dimensionless coordinates

d = depth of double diffusive layer in the z-direction

u, v, w = velocity components in the x, y, z directions

$w^* = wd/\kappa_T$ = dimensionless z-component of velocity

$z = 0,\ T = T_o,\ C = C_o,\ G_T = \partial T/\partial z = (T_1 - T_o)/d = (\Delta T)/d$

$z = d,\ T = T_1,\ C = C_1,\ G_C = \partial C/\partial M = (C_1 - C_o)/d = (\Delta C)/d$

$\Delta T, \Delta C$ = temperature and velocity differences, respectively, between the bottom and top boundaries.

$T^* = (T_o + G_T z - T)/(T_1 - T_o)$ = dimensionless temperature deviation

$C^* = (C_o + G_C z - C)/(C_1 - C_o)$ = dimensionless concentration deviation

$\nabla^2 = (\partial^2/\partial x^2) + (\partial^2/\partial Y^2) + (\partial^2/\partial Z^2)$

$Pr = \nu/\kappa_T$ = Prandtl number

$R_a = (g\,\alpha_T\,\Delta T\,d^3)/(\kappa_T\,\nu)$ = thermal Rayleigh number

and $R_C = (g\,\alpha_C\,\Delta C\,d^3)/(\kappa_T\,\nu)$ = salinity Rayleigh number

The postulated solutions are represented by:

$$w^* = w'd/k_T = f(X,Y)\,w^*(Z)\,e^{p\tau} \tag{A-32}$$

$$T^* = T'/(T_1 - T_o) = f(X,Y)\,\Theta(Z)\,e^{p\tau} \tag{A-33}$$

$$C^* = C'/(C_1 - C_o) = f(X,Y)\,\gamma(Z)\,e^{p\tau} \tag{A-34}$$

Separability of variables requires f(X, Y) to satisfy

$$(d^2f/dX^2) + (d^2f/dY^2) + \pi^2a^2f = 0 \tag{A-35}$$

where a is a constant from separation of variable, corresponding to a wave number. For rectangular cells

$$f(X,Y) = \cos(n_x\pi Xd/L_x)\cos(n_y\pi Yd/L_y) \tag{A-36}$$

where characteristic lengths L_x and L_y in the x, y directions and wave numbers

n_x and n_y satisfy:

$$\left(\frac{dn_x}{L_x}\right)^2 + \left(\frac{dn_y}{L_y}\right)^2 = a^2 \qquad \text{(A-37)}$$

For hexagonal cells, we have

$$f(X,Y) = \cos\frac{2n\pi d}{3L}\left(\sqrt{3}X+Y\right) + \cos\frac{2\pi nd}{3L}\left(\sqrt{3}X-Y\right) + \cos\frac{4\pi nd}{3L}Y \qquad \text{(A-38)}$$

where L is the length of a side and n is the wave number with

$$aL/d = 4n/3 \qquad \text{(A-39)}$$

Equations (A-23), (A-24), and (A-27) now take the form:

$$\frac{\partial}{\partial\tau}T^* - \nabla^{*2}T^* = -w^* \qquad \text{(A-40)}$$

$$\frac{\partial}{\partial\tau}C^* - k\,\nabla^{*2}C^* = -w^* \qquad \text{(A-41)}$$

where $k = \kappa_C/\kappa_T$,

$$\left(\frac{1}{Pr}\frac{\partial}{\partial\tau} + \frac{F^*}{Pr} - \nabla^{*2}\right)\nabla^{*2}w^* = -R_a\left(\frac{\partial}{\partial X^2} + \frac{\partial}{\partial Y^2}\right)T^* + R_c\left(\frac{\partial^2}{\partial X^2} + \frac{\partial^2}{\partial Y^2}\right)C^* \qquad \text{(A-42)}$$

and the Rayleigh numbers are:

$$R_a = \frac{g\alpha_T\, d^3}{\kappa_T\nu}(T_1 - T_o) = \frac{g\alpha_T G_T\, d^4}{\kappa_T\nu}$$

$$R_c = \frac{g\alpha_C\, d^3}{\kappa_T\nu}(C_1 - C_o) = \frac{\alpha_C(C_1 - C_o)}{\alpha_T(T_1 - T_o)}R_a = \frac{g\alpha_C G_C\, d^4}{\kappa_T\nu} \qquad \text{(A-43)}$$

Substitution of Eqs. (A-29) gives:

$$[p - (D^2 - \pi^2a^2)]\theta = -w^* \qquad \text{(A-44)}$$

$$[p - k(D^2 - \pi^2a^2)]\gamma = -w^* \qquad \text{(A-45)}$$

$$\left[\frac{p}{Pr} + \frac{F^*}{Pr} - (D^2 - \pi^2a^2)\right](D^2 - \pi^2a^2)w^* = R_a\pi^2a^2\theta - R_c\pi^2a^2\gamma \qquad \text{(A-46)}$$

where D = d/dZ, and the boundary conditions are:

$$w^*(0) = 0 = w^*(1) \qquad w^*(0) = 0 = w^*(1)$$

$$\theta(0) = 0 = \theta(1) \qquad \gamma(0) = 0 = \gamma(1)$$

The above basically follow Yih (1965). The following steps are now taken to obtain the basic relations for stability considerations:
Eliminating θ and γ from Eqs. (A-44) - (A-46), we get

$$\left[\frac{p}{Pr} + \frac{F^*}{Pr} - (D^2 - \pi^2a^2)\right](D^2 - \pi^2a^2)[p - (D^2 - \pi^2a^2)][p - k(D^2 - \pi^2a^2)] \quad *$$

$$= R_a\pi^2a^2[p - k(D^2 - {}^2a^2)](-w^*) - R_c\pi^2a^2[p - (D^2 - \pi^2a^2)](-w^*) \qquad \text{(A-47)}$$

For

$$w^* = \sin \pi mZ \qquad \text{(A-48)}$$

we have

$$(D^2 - \pi^2a^2)\, w^* = -(\pi^2m^2 + \pi^2a^2) \sin \pi mZ \equiv -b^2 \sin \pi mZ$$

$$(D^2 - \pi^2a^2)^2 w^* = b^4 \sin \pi mZ$$

$$(D^2 - \pi^2a^2)^3 w^* = b^6 \sin \pi mZ$$

$$(D^2 - \pi^2a^2)^4 w^* = b^8 \sin \pi mZ$$

Equation (A-47) now gives, after clearing up terms:

$$p^3 + \left(Pr + k + 1 + \frac{F^*}{b^2}\right) b^2p^2 + p\left[Pr + kPr + k + (k + 1)\frac{F^*}{b^2}\right] b^4$$

$$-(R_a - R_c)\frac{Pr\pi^2a^2}{b^2} + \left(kPr + \frac{kF^*}{b^2}\right)b^6 + (R_c - kR_a)Pra^2\pi^2 = 0 \qquad \text{(A-49)}$$

which is the same equation as in Veronis, Baines and Gill and Turner except for the F^* term. Difference in notations is aimed at using as many commonly used notations as possible. To facilitate analyses, we can, as in Baines and Gill (1969), make use of $p \equiv b^2q$, which gives

$$q^3 + \left[Pr + (k + 1) + \frac{F^*}{b^2}\right] q^2 + \left[(Pr + kPr + k) + (k+1)\frac{F^*}{b^2}\right.$$

$$\left. - (R_a^* - R_c^*)Pr\right] q + \left(k + k\frac{F^*}{b^2} + R_c^* - kR_a^*\right) Pr = 0 \qquad \text{(A-50)}$$

where

$$R_a^* = \frac{\pi^2 a^2 R_a}{b^6} , \quad R_c^* = \frac{\pi^2 a^2 R_c}{b^6} \tag{A-51}$$

We note that compared to the two-dimensional models,

$$b^2 = \pi^2(a^2 + m^2) \tag{A-52}$$

where m is the wave number of motion in the z-direction while a^2 now represents the wave numbers in the x-y directions such as given by Eq. (A-37) or Eq. (A-39).

As in the derivations of Veronis (1968), we arrive at the modified stability criteria as follows:

$$R_a^* = \left(R_c^*/k\right) + 1 + \left(F^*/b^2\right) \tag{A-53}$$

and

$$R_a^* = \frac{Pr + k + F^*/b^2}{Pr + 1 + F^*/b^2} R_c^* + (k + 1)\left(1 + \frac{k}{Pr}\right)$$

$$+ \left(F^*/b^2\right) \frac{1 + \frac{1 + 2k}{Pr} + \frac{k + 1}{Pr}\left(F^*/b^2\right)}{1 + Pr + \left(F^*/b^2\right)} \tag{A-54}$$

Both reduce to the result of Veronis (1968) for $F^* = 0$.

Calculation of F The force per unit volume acting on a fluid (f) by an immersed structure (w) is, for $F = F_{fw}$:

$$\rho_f F_{fw}\left(0 - U_f\right) = -\rho_w F_{wf}\left(U_f - 0\right) \tag{A-55}$$

For the grid work in Fig. 5 with depth d, wall material density $\overline{\rho_w}$, $\rho_f = \rho$, and spatial density of grid p_w, we have:

$$F_{wf} = (\text{shear stress})(\text{area})(\text{mass})^{-1}$$

$$\sim \left[2\mu\, U_f/(w/2)\right]\left[4wd\right]\left[2wd\delta\overline{\rho}_w\right]^{-1}$$

$$= 8\mu/\delta w\overline{\rho}_w \tag{A-56}$$

since $\rho_w/\overline{\rho}_w \sim \delta/w$, $\nu = \mu/\rho_f$, we get

$$F = F_{fw} = \left(\rho_w/\rho_f\right) F_{wf} \sim 8\nu/w^2 \tag{A-57}$$

APPENDIX B

CONVERSIONS FOR COMPARISON TO EXPERIMENTAL RESULTS

In order to compare to the results of Zangrando (1979), not only the notations have to be converted, but also the parameters as outlined below:

For plotting into Fig. 1, k_1 and k_2 in Zangrando are converted to R_a and R_c.

$$R_a = k_1(Pr + k)(1 + k)/Pr$$

$$R_c = k_2(Pr + 1)(1 + k)/Pr$$

or

$$k_1/k_2 = R_a(Pr + 1)/R_c(Pr + k)$$

The dimensionless velocity W is converted to physical velocities via

$$w = (\kappa_T/d)W$$

The conversions were made according to physical quantities given by Zangrando (60°C)

ρ, density	1.0887×10^3 kg/m^3
c, specific heat	3.57×10^3 J/kgC
κ, thermal conductivity	6.37×10^{-1} W/mC
ν, kinematic viscosity	5.81×10^{-7} m^2/s
κ_T, thermal diffusivity	1.64×10^{-7} m^2/s
κ_C, solute diffusivity	3.3×10^{-9} m^2/s
α_T, $-(\partial\rho/\partial T)_p/\rho$	5.3×10^{-4}/C
α_C, $(\partial\rho/\partial C)_p/\rho$	6.98×10^{-3} by wt.

APPENDIX C

EXAMPLE OF EXTRACTION OF ENERGY FROM A SOLAR POND

We take a one-acre pond of 40 m x 100 m with a 2 m bottom convective layer. Heat is collected over the spring and summer months to a water temperature of 88°C (190°F) for use in supplying part of the heat for grain drying from October 1 for one month in a water (brine) tube heat exchanger for heating 250,000 cfm of air from 15.5°C (60°F) to 24°C (75°F) at the beginning of this one month period. Seventy-five gpm of salt water will be extracted for this purpose. We shall use this example to demonstrate the desirability of maintaining a longitudinal stratification to assure a high availability of energy from a solar pond.

Heat Exchanger. The heat exchanger tubes are as shown in Fig. C.1 with the design given for 2 heat exchangers, each of 20 ft length.

No. of tubes in each row - 40

Frontal area: 20 x 41 x 1.232 = 84.19 ft

Free flow area: 37.80 ft^2

Air Side	Water side
Air velocity 55.11 ft/s	Water velocity 1.225 ft/s
Reynolds No., Re 7405	Re = 8039
Heat transfer coefficient h_a = 30.42 Btu/ft^3hrF	h_w = 356.9 Btu/ft^3hrF
Heat transfer area, A_a = 3883	A_w = 4650

$UA_a = 6.9 \times 10^4$

Overall heat transfer coefficient, U = 17.8

No. of heat transfer units, NTU_{max} = 4.695 for 4 path

Effectiveness = 0.81 = ε

(Kays and London, 1954)

Heat Transfer Relations. To determine the variable temperature performance, we have the following relations:

$$\text{Heat Flow} = \varepsilon \dot{m}_w (T_{win} - T_{ain})$$
$$= \dot{m}_w c_{pw} (T_{win} - T_{wout})$$
$$= \dot{m}_a c_{pw} (T_{aout} - T_{ain})$$

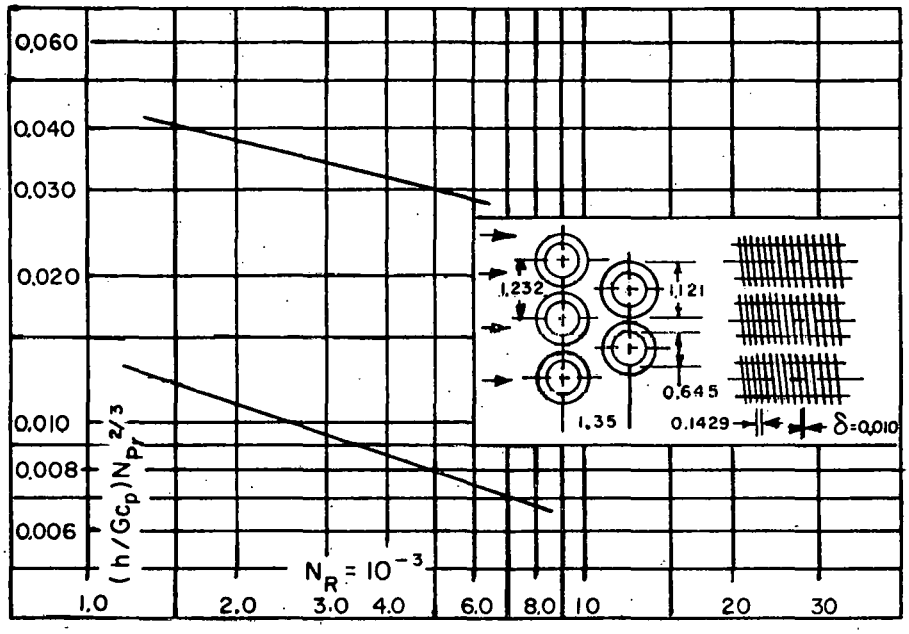

FINNED CIRCULAR TUBES
SURFACE CF-T.0 - 5/SJ
(Data of Jameson)

Tube outside diameter - 0.645 in.
Pin pitch - 7.0 per inch
Flow passage hydraulic diameter - $4r_h$ = 0.0219 ft.
Pin thickness - 0.010 in.
Free-flow area/frontal area - σ = 0.449
Heat transfer area/total volume - α = 82 ft^2/ft^3
Pin area/total area - 0.830

Note: Minimum free-flow area is in spaces transverse to flow. These data are included in this compilation because they include compact arrangements of interest that are not adequately covered by Figs. 92-95. (Kays & London, 1954)

Fig. C-1. Finned Circular Tubes (Kays & London, 1954)

$$\Delta T_1 = T_{win} - T_{aout}$$

$$\Delta T_2 = T_{wout} - T_{ain}$$

Logarithmic temperature difference = $(\Delta T_1 - \Delta T_2)/\ell n(\Delta T_1/\Delta T_2)$

Heat Flow = $UA\Delta T_m$

where $\dot{m}_w$ is the extraction rate of brine, $\dot{m}_a$ is air flow rate, c_p's are the specific heats of water and air respectively. In the mixing mode at step (i + 1)

$$T_{m(i+1)} = \frac{w_{cold}\ T_{wout(i)} + w_{warm}\ T_{mi}}{}$$

$$w_{cold} = \dot{m}_w \sum \Delta t$$

where $\sum\Delta t$ is the time from beginning of extraction. The pond content w is given by

$$w_{cold} + w_{warm} = w$$

Numerical integration gives Fig. C.1.

ACKNOWLEDGEMENT

The authors would like to acknowledge Professor B. T. Chao for many stimulating discussions. We would like to thank Dr. John R. Hull for his critical review of this report.

REFERENCES

Baines, P. G., and Gill, A. E., 1969, "On Thermohaline Convection with Linear Gradients," J. Fluid Mech. 37, 289-306

Corrsin, S., and Kollmann, W., 1971, "Preliminary Report on Sheared Cellular Motion as a Qualitative Model of Homogeneous Turbulent Shear Flow," Turbulence in Internal Flows, a 1976 Project SQUID Workshop (S. N. B. Murthy) Hemisphere Pbul. Corp., Washington, D.C.

Dickinson, W. C., Clark, A. F., and Iantuono, A., 1976, "Shallow Solar Ponds for Industrial Process Heat: The ERDA-SOHIO Project," Proc. Jt. Conf. of the Int. Solar Energy Soc., Am. Sect. and Solar Energy Soc. of Canada, Winnipeg, Canada, Vol. 5, pp. 117-141

Dubois, M., and Berge, P., 1978, "Experimental Study of the Velocity Field in Rayleigh-Benard Convection," J. Fluid Mech., 85 (4), pp. 641-653

Elata, C., and Levin, O., 1965, Proc. IAHR 11th International Congress, Leningrad, Vol. II, pp. 2-3.

Elder, J. W., 1969, "Numerical Experiments with Thermohaline Convection," Phys. Fluids 12(II), pp. 194-197

Hull, J. R., 1980, "Membrane Stratified Solar Ponds," Solar Energy (in press).

Kato, H., and Phillips, O. M., 1969, "On the Penetration of a Turbulent Layer into Stratified Fluid," J. Fluid Mech. 37, pp. 643-655

Kays, W. M., and London, A. L., 1954, "Compact Heat Exchangers - A Summary of Basic Heat Transfer and Flow Friction Design Data," Tech. Report No. 23, Contract N6-ONR-251, Task Order 6 (NR-065-104) for ONR, Stanford University

Lin, E. I. H., Sha, W. T., and Soo, S. L., 1979, "Stability Consideration and a Double-Diffusive Convection Model for Solar Ponds," Tech. Memo ANL-CT-79-34, April

Linden, P. F., and Shirtcliffe, T. G. L., 1978, "The Diffusive Interface in Double-Diffusive Convection," J. Fluid Mech., Vol. 87, part 3, 417-432

Nield, D. A., 1967, "The Thermohaline Rayleigh-Jefferys Problem," J. Fluid Mech. 20, 545-558

Nielsen, C. E., 1976, "Experience with a Prototype Solar Pond for Space Heating," Proc. Jt. Conf. of the Int. Solar Energy Soc., Am. Sect. and Solar Energy Soc. of Canada, Winnipeg, Canada, Vol. 5, pp. 169-182

Nielsen, C. E., and Rabl, A., 1976, "Salt Requirement and Stability of Solar Ponds," Proc. Jt. Conf. of the Int. Solar Energy Soc., Am. Sect. and Solar Energy Soc. of Canada, Winnipeg, Canada, Vol. 5, pp. 183-187

Nielsen, C. E., 1978, "Equilibrium Thickness of the Stable Gradient Zone in Solar Ponds," Proc. Am. Sec. Int. Solar Energy Soc., Denver, Colorado, Vol. 2.1, pp. 932-935

Nielsen, C.E., 1979, "Nonconvective Salt-Gradient Solar Ponds," Solar Energy Handbook (W. C. Dickinson, P. N. Cheremisnoff, ed.) Marcel Dekker, Inc.

Plesset, M. S.., 1974, "Bubble Dynamics and Cavitation Erosion," in Finite-Amplitude Wave Effects in Fluids, IPC Science and Technology Press, Ltd.

Soo, S. L., 1967, "Fluid Dynamics of Multiphase Systems," Blaisdell, Ch. 2.4, 2.5

Turner, J. S., 1968, "The Behavior of a Stable Salinity Gradient Heated from Below," J. Fluid Mech. 33, 183

Turner, J. S., 1973, Buoyancy Effects in Fluids, Cambridge University Press

Veronis, G., 1968, "Effect of a Stabilizing Gradient of Solute in Thermal Convection," J. Fluid Mech. 34, 315-336

Wyatt, L. R., 1978, "The Entrainment Interface in a Stabilized Fluid," J. Fluid Mech. 86, pp. 293-311

Weinberger, H., 1964, "The Physics of the Solar Pond," Solar Energy, Vol. 8, No. 2, pp. 45-56

Yih, C. S., 1965, Dynamics of Nonhomogeneous Fluids, MacMillan

Zangrando, F., 1979, "Observation and Analysis of a Full-Scale Experimental Salt Gradient Solar Pond," Ph.D. Thesis, Dept. of Physics, University of New Mexico, May

Distribution for ANL-CT-80-23

Internal:

C. E. Till
J. J. Roberts
W. W. Schertz
A. I. Michaels
J. J. Peerson
R. L. Cole
R. S. Zeno
G. S. Rosenberg
P. R. Huebotter
W. T. Sha (20)
Y. S. Cha (6)
B. C. Chen
T. H. Chien
H. M. Domanus
J. R. Hull
K. V. Liu (6)
C. C. Miao
R. C. Schmitt
V. L. Shah
M. R. Sims
S. P. Vanka
C. I. Yang
ANL Contract File
ANL Libraries (2)
TIS Files (6)

External:

DOE-TIC, for distribution per UC-62a (321)
Manager, Chicago Operations and Regional Office, DOE
Chief, Office of Patent Counsel, DOE-CORO
S. Sargent, DOE-CORO
President, Argonne Universities Association
Components Technology Division Review Committee:
- F. W. Buckman, Consumers Power Co.
- P. F. Cunniff, U. Maryland
- R. A. Greenkorn, Purdue U.
- W. M. Jacobi, Westinghouse Electric Corp., Pittsburgh
- M. A. Schultz, North Palm Beach, Fla.
- A. Sesonske, Purdue U.
- J. Weisman, U. Cincinnati

Office of Solar Applications, DOE:
- W. Auer
- J. Crane
- F. Deserio
- J. Dollard
- J. Hale
- R. Hassett
- F. Morse, Director
- J. Rannels
- S. Schweitzer

P. Flynn, Ohio Agricultural R&D Center, Wooster
F. Glaski, San Francisco Operations Office, DOE
C. Kooi, Palo Alto
R. LeChevalier, Science Applications, Inc., Golden
K. Meyer, Los Alamos Scientific Lab.
C. Nielsen, Ohio State U.
T. Ochs, Desert Research Inst., Boulder City, Nev.
S. L. Soo, U. Illinois, Urbana (6)
R. Talwar, Mid-American Solar Energy Complex, Minneapolis
L. Wittenberg, Monsanto Research, Miamisburg
F. Zangrando, Solar Energy Research Institute